ORIGINAL ARTICLE

lajss.org© Latin American Journal of Solids and Structures

www.lajss.org

Behavior of Macro-Synthetic Fiber-Reinforced High-Strength Concrete Beams Incorporating *Bacillus subtilis* Bacteria

Amr Ghoniem[a*], Hilal Hassan[a], Louay Aboul-Nour[a]

[a] Structural Engineering Department, Faculty of Engineering, Zagazig University, Postal Code: 44519, Egypt.
Email: amr.gamal.87@gmail.com, habdelkader@zu.edu.eg, laran@zu.edu.eg

* Corresponding author

https://doi.org/10.1590/1679-78256378

Abstract

High-strength concrete incorporating macro-fiber combines high compressive strength of the matrix, strain-hardening, and multiple crack characteristics. Also, calcite sediment remediation bacterial techniques can enhance the mechanical properties, reduce concrete deterioration, and prevent corrosion of steel reinforcement in both the short-term and long-term. In this paper, The *Bacillus subtilis* bacteria at an optimum dosage of 10^5 cells/ml of mixing water was incorporated into M60 and M80 concrete strengthened with 0.5% macro synthetic-fiber content. The performance of 32 simply supported reinforced concrete beams with rectangular-section were evaluated numerically using ANSYS. In this study, the properties of matrix components are considered for different geometric sizes as slender and short beams with different longitudinal reinforcement ratios. The results showed that the bacterial participation in fibrous concrete beams had more significant enhancement in the initial cracking load, ultimate load, moment capacity ratio, ductility ratio, and flexural toughness compared to associated conventional concrete.

Keywords

Bacillus subtilis; High-Strength; Fiber; Performance; Non-conventional Concrete; Numerical.

Graphical Abstract

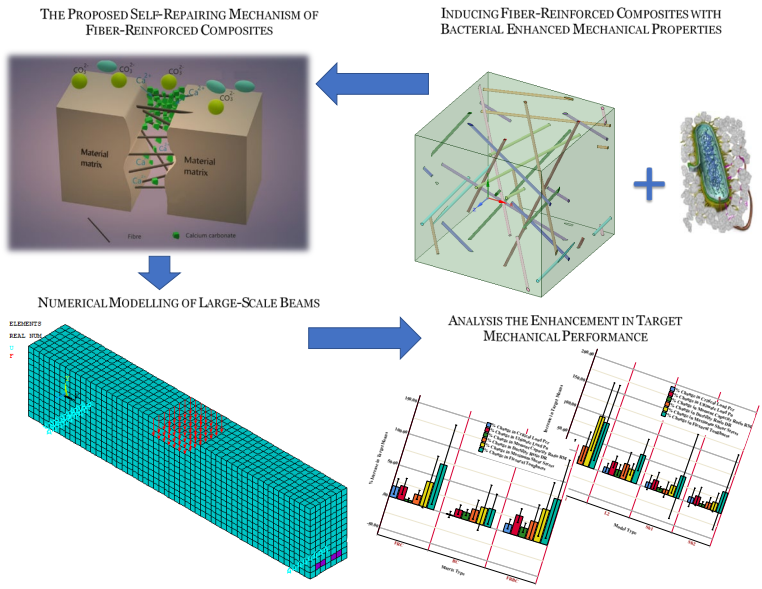

Received December 30, 2020. In revised form February 10, 2021. Accepted February 11, 2021. Available online February 12, 2021.
https://doi.org/10.1590/1679-78256378

1 INTRODUCTION

The cracks in concrete structures are predictable due to deterioration throughout their service life through various load combination factors. For that reason, there is a need for a product that generates multiple micro cracks and repairs it to prevent the cracks from propagating. This article deals with the Fiber-Reinforced Bacterial Concrete (FRBC), which is defined as fiber-reinforced concrete self-repaired by bacteria. The produced FRBC presents a further step development of construction materials with both performance and sustainable service life (Karimi and Mostofinejad, 2020). Adopting the self-repairing mechanism produces smart infrastructure systems. Smart structures can provide a unique response of sensing and action that make concrete sustainable, durable, and protected against any aggressive environments without expensive maintenance (Li et al., 2019; Zhang et al., 2020). Also, the crack treatment affects the behavior of Fiber-Reinforced Concrete (FRC) beams due to improved adhesion between the fiber and the matrix. The increased frictional shear stress during the pull-out allows the full fiber anchorage utilization without the fiber rupture (Di Maida et al., 2018). The short macro-fiber distributed randomly in the matrix can bridge the crack width and also improve both fresh and hardened mechanical properties (Alberti et al., 2020).

The carbonate participation technique can regain original mechanical that enhances strength and durability properties in the short-term and long-term (Hizami Abdullah et al., 2018). However, the fiber could affect the concrete tensile strength only, bacterial self-repairing can enhance both compressive and tensile strength of Bacterial Concrete (BC). The $CaCO_3$ bacterial participation can heal both micro/macro-cracks of the cracked section and voids of the uncracked section by reducing the ingress of moisture and aggressive elements, which eventually lead to concrete deterioration (Micelli et al., 2019; Griño et al., 2020). Bacterial self-repairing can enhance the early-age concrete compressive and tensile strengths. The compressive strength of concrete was optimized at the *B. subtilis* bacteria cell concentration of 10^5 cells/ml of mixing water (increased by an average value of 23% at age 28 days). Moreover, the split tensile strength improved in a range of (13.7 - 25.3%) (Ghoneim et al., 2020).

Conventional Concrete (CC) becomes more brittle and has very low flexure or shear capacities when its compressive strength increases. To reduce these side effects, FRC has arisen as an Engineering Cementitious Composites (ECC). The higher fiber content may cause accumulation in the concrete. Therefore, the moderate fiber content should be less than 4% to make sure an adequate balance between obtaining post cracking behavior and the workability of fresh concrete benefits (Hasan et al., 2019). Both the Microbially Induced Calcite Precipitation (MICP) and fibers have no side effects on the cement specimen containing admixtures (Termkhajornkit et al., 2009; Athiyamaan and Ganesh, 2017). For improving self-healing capacity, the combination of fibers with cement replacement is recommended (Guerini et al., 2018). High Strength Concrete (HSC) with a strength more than 60 MPa could be produced through the addition of cement replacements frequently as Silica Fume (SF), fly ash, Ground Granulated Blast Furnace Slag (GGBS), limestone powder, and metakaolin (MK). HSC can reduce structural member size, enhance density and permeability, but its durability and serviceability enhancement need more requirements to resist sulfate, freeze-thaw, abrasion, low alkali-aggregate reactions, and embedded steel corrosion (Ayub et al., 2014).

Coupled effects of macro fibers and bacteria on early-age characteristics of concrete are mentioned in the literature (Feng et al., 2019; Ganesh et al., 2019). However, studies on the short-term performance of concrete beams made with bacteria and different fiber admixtures are very scarce. The authors believe that this fusion generates the development of HSC mechanical properties and structural behavior by achieving high strength, strain hardening, and multiple microcracking characteristics. The 32 admixtures were carried out to judge the properties of the FRBC beams with higher concrete grade (M60 & M80) and investigate its performance, initial cracking, and failure behavior.

2 STUDY PROCEDURE

There is a multiscale modeling issue ranging from the fiber with a few micrometers in diameter to the structural dimension in meters. The link between the length scales using either the hierarchical approach or the homogenization approach eliminates the scale problem in the Finite Element (FE) modeling. Although the evaluation of organisms curing condition is difficult numerically, the crack opening width ζ for fibrous concrete should stay within an ever-experienced limit of B. subtilis rehabilitation incorporated to close cracks up to 0.46 mm (Wiktor and Jonkers, 2011).

2.1 Samples Description

The beams proposed with varying geometry are tested under a monotonic three-point loading system as shown in Figure 1. The rectangular beam sections configured with no stirrups by different geometrical parameters such as; clear span length l_n, shear-span to depth ratio a/d (the shear-span a is half of the beam span l_n in a three-point loading setup), width b, height h, depth d, and flexure singly reinforcement ratio ρ.

Beams with shear-span to depth ratios a/d from 1.0 to 2.5 are referred to as “short”, while those with a/d from 2.5 to about 6.0 are referred to as “slender” (a slender beam geometry has reduced beam height, increased span length, or both) (MacGregor and Wight, 2012). To consider the influence of beams size on the results, two major types of beams in terms of slenderness were selected to be investigated in this study since they have different failure mechanisms (slender beams fail due to the propagation of flexure-shear cracks while short beams fail more due to the propagation of web-shear cracks). Table 1 presents the details of the four geometry model types L1, L2, Sh1, and Sh2. In the notation used for the beam titles, the letter ‘L’ denotes long and is used for slender beams (a/d = 3.5) while ‘Sh’ represents short (a/d = 2.3). Numbers 1 and 2 indicate the first phase and second phase with flexural reinforcement ratio ρ equals 2.15% and 3.18%, respectively.

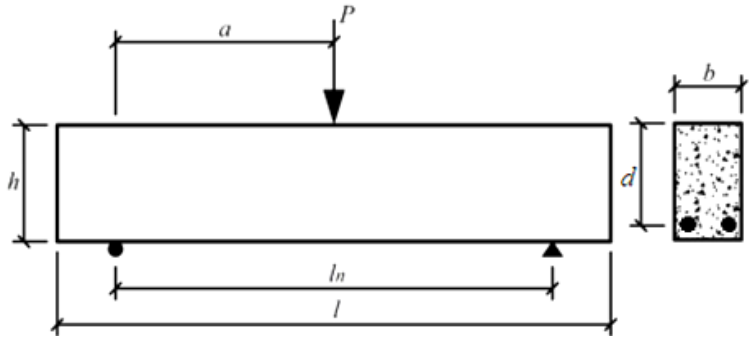

Figure 1: Schematic Outline of Beam Configuration.

Table 1 Geometry Details and Reinforcement Arrangements of the Concrete Beams.

Model Type	a/d	l_n [mm]	b [mm]	h [mm]	d [mm]	ρ [%]
L1	3.5	2820	280	460	400	2.15
L2		2310	230	390	330	3.18
Sh1	2.3	1820	280	460	400	2.15
Sh2		1500	230	390	330	3.18

The steel bars idealized to have compressive and tensile elastic perfectly plastic behavior with a modulus of elasticity E_s equals 2.1×10^5 MPa, Poisson’s ratio v equals 0.3, and yield stress f_y equals 420 MPa. The modeled beam load (500 kN) and the hinged roller restraints are represented in Figure 2.

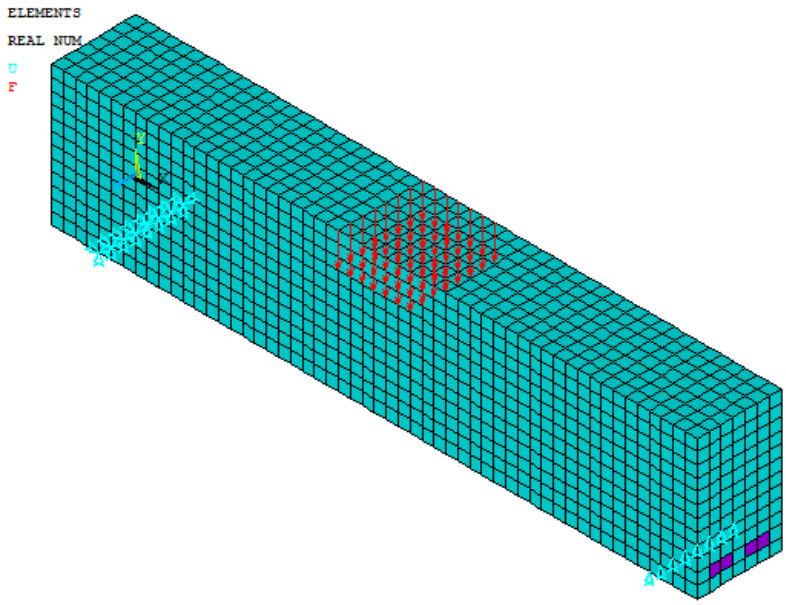

Figure 2: Modeled Beam Load, Restraints, and Real Constant Configuration (The Beam Elements are Distinguished by Real Constant Color where the Purple Color for Smeared Element appeared in the cross-section).

The 32 full-scale reinforced concrete (RC) beams were analyzed under a monotonic three-point loading system. The study classified the beams into three matrix types (fiber-reinforced concrete FRC, bacterial concrete BC, fiber-reinforced bacterial concrete FRBC). The scheme of specimen sets is outlined in Figure 3.

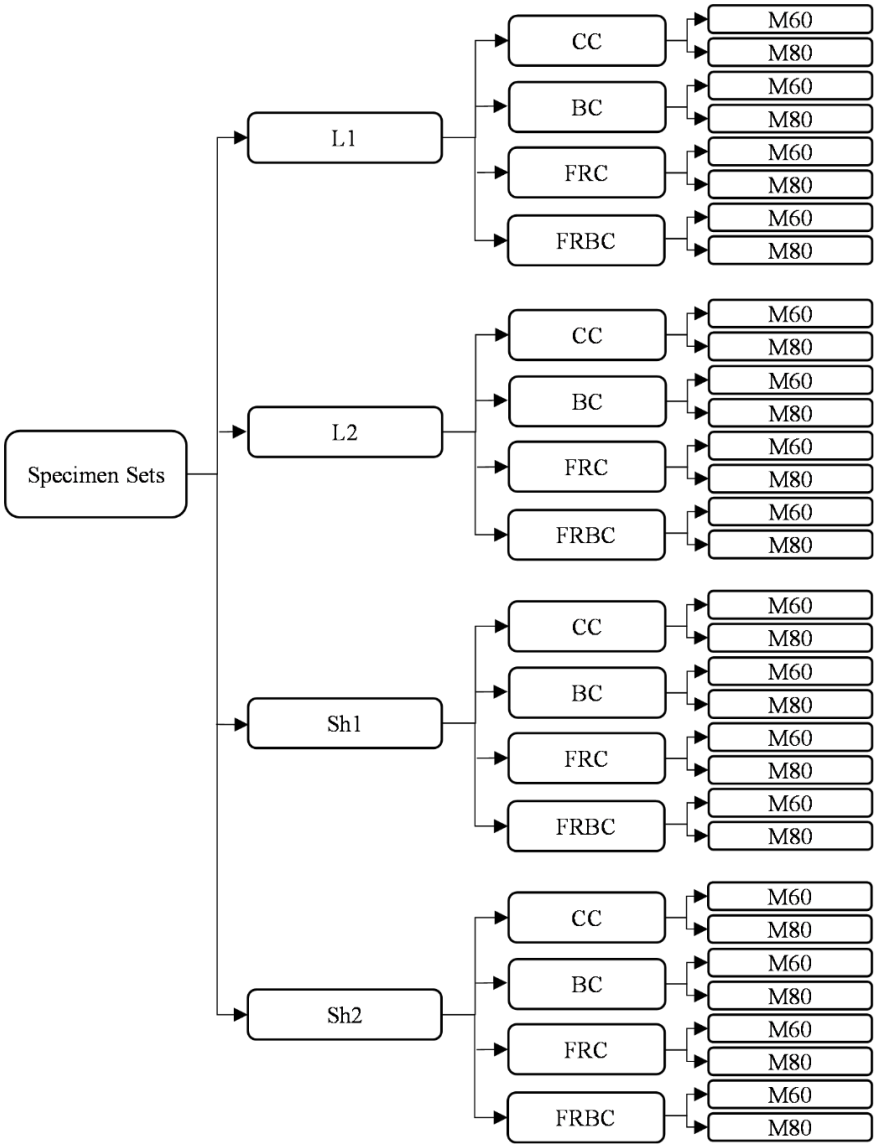

Figure 3: Scheme of Specimen Sets (The test variables are "Geometry Model Type - Matrix Type – Concrete Grade").

2.2 Material Properties

To provide reliable inputs for the study, the properties of matrix integrated materials are considered based on previous experimental literature. For both high strength M60 & M80 concrete grades, the matrix properties are characterized by early-age concrete properties after 28 days as mentioned by Rao et al., 2017. For the present study, Bacillus subtilis JC3 is distinguished as aerobic alkaliphilic spore-forming bacteria. The growth medium used is based on peptone, NaCl, yeast extract (Rao et al., 2017).

The straight macro synthetic fiber has unit diameter d_f equals 433 µm, aspect ratio $AR_f = l_f / d_f$ equals 90, specific gravity equals 0.97 g/cm^3, elastic modulus E equals 73000 MPa, Poisson's ratio v equals 0.422, and ultimate tensile strength equals 2580 MPa. The fiber was incorporated into the concrete mixture with 0.5% fiber content and the optimum cell concentration of *B. subtilis* equals 10^5 cells/ml of mixing water. The uniaxial crushing stress set in the fibrous concrete is similar to the non-fibrous concrete pre peak compressive stress f_{cu} as shown in Table 2. The effective Young's modulus and the Poisson's ratio of composites could be computed using the properties of their integrated materials. This could be performed through the ANSYS Material Designer as an integrated component system in the ANSYS package using the homogenization or unit cell approach. The unit cell is a repeated cell or a typical Representative Volume Element (RVE) proposed in Figure 4 for predicting the equivalent homogeneous material properties.

Table 2 Properties and Initial Material Input Parameters of the Concrete Beams.

Target ID	E [MPa]	v	f_{cu} [MPa] ($f_c' = f_{cu}/1.2$)	f_t [MPa]	
				Stage 1	Stage 2
CC-M60	38700	0.18	72.61 (60)	4.63	4.63
CC-M80	43600	0.18	93.8 (78.16)	4.88	4.88
FRC-M60	38835	0.1815	72.61 (60)	4.76	5.19
FRC-M80	43729	0.1816	93.8 (78.16)	5.02	5.47
BC-M60	44100	0.18	94.21 (78.5)	5.63	5.63
BC-M80	50900	0.18	119.2 (99.33)	5.76	5.76
FRBC-M60	44228	0.1816	94.21 (78.5)	5.79	6.31
FRBC-M80	51015	0.1817	119.2 (99.33)	5.93	6.46

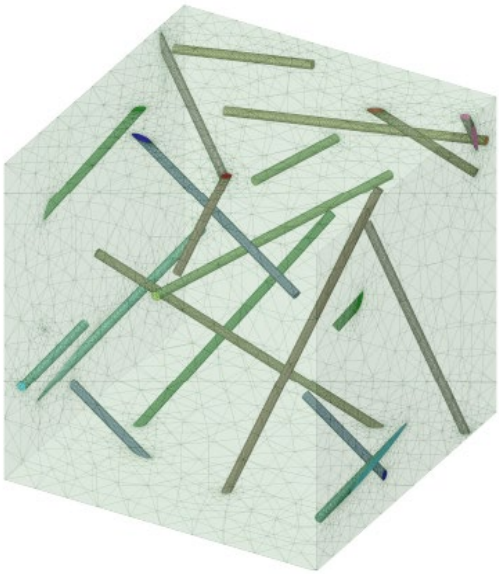

Figure 4: Typical Representative Volume Element (RVE).

The concrete linear isotropic ANSYS input data properties are valid for each beam geometry group L1, L2, Sh1, and Sh2 as illustrated in Table 2, where the target sample notation is "Matrix Type - Concrete Grade". However, the elastic modulus and Poisson's ratio of fibrous composites are the homogenized RVE characteristics, the total tensile stress ft determined by the literature approach in Eq. (1).

Both the Variable Engagement Model (VEM) and the Simplified Diverse Embedment Model (SDEM) are the recommended models to determine the total FRC tensile stress f_t (Carnovale, 2013). The total FRC tensile stress mentioned in Eq. (1) consists of three terms, as follows: (i) the frictional bond stress in the macro synthetic fiber f_f presented by modifying SDEM has given in Eq. (2), (ii) the mechanical anchorage stress f_{eh} (the smooth straight fiber has no mechanical anchorage component), and (iii) the matrix tensile cracking strength f_{ct}. The crack opening width ζ should stay within an ever-experienced limit of *B. subtilis* rehabilitation incorporated to close cracks up to 0.46 mm as recommended in the literature (Wiktor and Jonkers, 2011).

$$f_t = \left(f_f + f_{eh}\right) + \left(f_{ct}\right) \tag{1}$$

$$f_f = \frac{V_f l_f}{d_f} \tau_{f,\max} \alpha_f K_{st} \left(1 - \frac{2\zeta}{l_f}\right)^2 \tag{2}$$

In these expressions; V_f is the fiber content (%), l_f is the fiber length (mm), d_f is the fiber diameter (mm), $\tau_{f,\,max}$ is the fiber maximum bond strength constant (equals 0.6 of the concrete matrix (Won et al., 2006)), and α_f is the fiber orientation factor as a function of member thickness b and height h in Eq. (3) (Oh, 2011).

For surveying the after-cracking behavior, two stages are considered with the K_{st} coefficient: (i) early-stage 1 for the elastic fiber behavior at a small crack width; and (ii) latterly stage 2 for the plastic fiber behavior at large crack width. This coefficient in Eq. (4) is a function of the straight fiber slip S_f at $\tau_{f,max}$ that was consistently equal to 0.01 mm.

$$\alpha_f = 0.5 + \frac{0.13}{\left(\frac{bh}{l_f^2}\right)^{1.12}} + 0.087\left[\left(\frac{l_f}{b}\right)^{1.12} + \left(\frac{l_f}{h}\right)^{1.12}\right] \tag{3}$$

$$K_{st} = \begin{cases} \dfrac{0.67\zeta}{3S_f} & \zeta < S_f \\ 1 - \sqrt{\dfrac{\zeta}{S_f}} + \dfrac{0.67}{3}\sqrt{\dfrac{\zeta}{S_f}} & \zeta \geq S_f \end{cases} \tag{4}$$

For the non-fibrous concrete, the uniaxial tensile cracking stress f_t is set into the investigated values in the literature (Rao et al., 2017). While the addition of smooth macro synthetic fiber increases the tensile cracking strength f_t as in Table 2. According to the SDEM, Eqs. (1) to (4) implies the formulations for both stage 1 ($\zeta > 0.01$ mm) and stage 2 ($\zeta \geq 0.01$ mm). The K_{st} coefficients are equal to 0.2 and 0.885 for stage 1 and stage 2, respectively. The member geometry has little effect on the fiber orientation factor α_f and equals 0.52.

The multilinear isotropic stress-strain material properties of the compressive models based on the experiments are depicted in Figure 5. The study selects some of the expressions as Carreira and Chu model, 1985 (Carreira and Chu, 1985) and Lu and Zhao model, 2010 (Lu and Zhao, 2010) to describe the stress-strain relationship of non-fibrous conventional and bacterial concrete with different concrete strength ranges. On the other hand, to calculate the actual uniaxial compressive stress-strain relationship of fibrous concrete, the expressions of Oliveira Júnior et al. model, 2010 (Júnior et al., 2010), Wen-Cheng et al. model, 2015 (Liao et al., 2015), and Ayub et al. model, 2018 (Ayub et al., 2018) are presented.

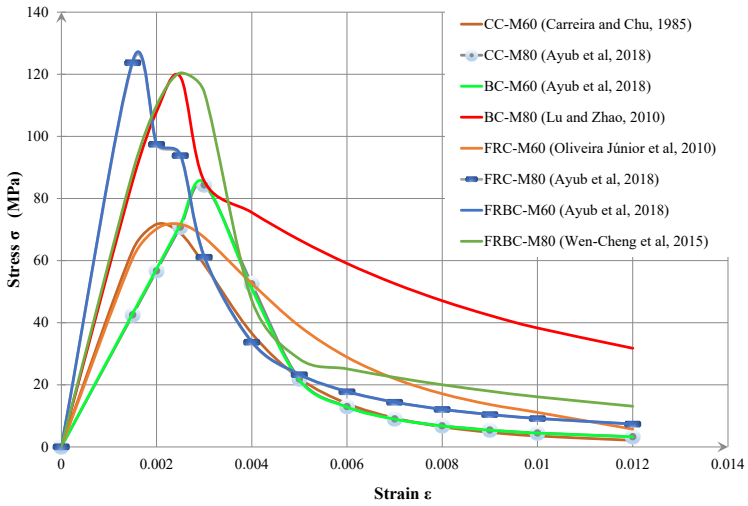

Figure 5: Multilinear Isotropic Stress-Strain Material Properties of the Tested Concrete Beams Based on the Literature Experiments (*Carreira and Chu, 1985*) (*Ayub et al., 2018*) (*Lu and Zhao, 2010*) (*Júnior et al., 2010*) (*Liao et al., 2015*).

In addition, the inelastic plasticity is defined using the Willam and Warnke model by constants such as the typical shear transfer coefficients for an open crack β_t and a closed crack β_c. For the non-fibrous concrete, the β_t and β_c coefficients were set to 0.25 and 0.7, respectively. For the fibrous concrete, the shear transfer at the cracks depends on the pull-out mechanism in the matrix-fiber interaction. For V_f = 0.5%, the β_t and β_c coefficients were set by linear interpolation as 0.31 and 0.73, respectively, based on the previous investigations (Thomas and Ramaswamy, 2006; Thomas and Ramaswamy, 2007).

3 RESULTS

For providing an in-depth understanding of the combined effect of bacteria and fibers on the behavior of simple RC beams, an extensive parametric study was designed. The numerical modeling results of the concrete beam specimen at both fiber elasticity-plasticity stages are shown in Table 3, these two stage results are as follows:

(i) Stage 1, the elastic fiber behavior at a small crack width was used for determining the fiber elastic initial cracking load $P_{cr,e}$, the mid-span flexure $M_{cr,e}$ that occurs from the existing forces with neglecting the own weight of beams, and the deflection $\delta_{cr,e}$.

(ii) Stage 2, the plastic fiber behavior at large crack width led to determine the fiber plastic ultimate load $P_{u,p}$, the mid-span flexure $M_{u,p}$, the maximum nodal XY shear strength v_{fc}, and the flexural toughness (the area under the flexural load deflection curve obtained from a specimen static test up to a specified deflection) as an indication of the material energy absorption capability, and the deflection $\delta_{u,p}$. Hence, the ductility ratio ($DR = \delta_{u,p}/\delta_{cr,e}$) and the moment capacity ratio ($RM = M_{u,p}/M_{cr,e}$) could be calculated.

Table 3 Numerical Results and the Change percentage Related to the Associated CC.

Specimen ID	$P_{cr,e}$ [kN]	$P_{u,p}$ [kN]	RM	DR	v_{fc} [MPa]	Flexural Toughness [kN.mm]
	(% Change)	(% Change)	(% Change)	(% Change)	(% Change)	(% Change)
L1-CC-M60	108.40	103.40	0.95	0.81	0.72	24.40
L1-BC-M60	139.50 (28.69)	134.54 (30.12)	0.96 (1.11)	0.87 (7.46)	0.94 (29.75)	50.00 (104.92)
L1-FRC-M60	110.10 (1.57)	113.91 (10.16)	1.03 (8.46)	0.95 (16.42)	0.79 (10.12)	30.20 (23.77)
L1-FRBC-M60	131.72 (21.51)	149.54 (44.62)	1.14 (19.02)	1.25 (54.4)	1.86 (157.8)	73.00 (199.18)
L1-CC-M80	118.90	113.91	0.96	0.91	0.79	36.20
L1-BC-M80	126.40 (6.31)	126.72 (11.25)	1.00 (4.64)	1.05 (15.60)	2.03 (155.8)	45.40 (25.41)
L1-FRC-M80	113.90 (-4.21)	126.72 (11.25)	1.11 (16.13)	1.25 (37.12)	1.83 (130.9)	52.10 (43.92)
L1-FRBC-M80	128.14 (7.77)	158.14 (38.83)	1.23 (28.82)	1.62 (78.10)	1.59 (100.4)	86.10 (137.85)
L2-CC-M60	73.28	78.28	1.07	1.10	1.13	21.20
L2-BC-M60	88.02 (20.12)	95.71 (22.27)	1.09 (1.79)	1.17 (5.58)	1.32 (16.58)	35.10 (65.57)
L2-FRC-M60	80.92 (10.43)	90.94 (16.17)	1.12 (5.20)	1.19 (8.14)	1.25 (10.67)	28.00 (32.08)
L2-FRBC-M60	88.62 (20.93)	112.42 (43.61)	1.27 (18.75)	1.35 (22.46)	1.54 (36.78)	40.40 (90.57)
L2-CC-M80	80.94	95.94	1.19	1.22	1.32	36.70
L2-BC-M80	84.48 (4.38)	108.91 (13.52)	1.29 (8.76)	1.56 (27.84)	1.49 (13.30)	42.60 (16.08)
L2-FRC-M80	85.43 (5.55)	125.43 (30.74)	1.47 (23.87)	1.89 (54.87)	1.72 (30.63)	67.60 (84.20)
L2-FRBC-M80	83.62 (3.31)	123.14 (28.35)	1.47 (24.24)	1.91 (56.43)	1.69 (28.43)	52.50 (43.05)
Sh1-CC-M60	144.53	139.54	0.97	0.90	1.12	15.80
Sh1-BC-M60	188.16 (30.19)	193.16 (38.43)	1.03 (6.33)	1.14 (26.32)	1.54 (38.08)	44.70 (182.91)
Sh1-FRC-M60	151.07 (4.53)	160.16 (14.78)	1.06 (9.81)	0.98 (8.60)	1.28 (14.75)	21.20 (34.18)
Sh1-FRBC-M60	178.64 (23.60)	190.94 (36.84)	1.07 (10.71)	0.99 (9.50)	1.53 (36.92)	28.30 (79.11)
Sh1-CC-M80	165.16	165.16	1.00	1.10	1.32	33.30
Sh1-BC-M80	170.86 (3.45)	175.86 (6.48)	1.03 (2.93)	1.24 (13.32)	1.51 (14.42)	33.2 (-0.30)
Sh1-FRC-M80	156.07 (-5.50)	170.86 (3.45)	1.09 (9.48)	1.21 (10.01)	1.37 (3.80)	31.2 (-6.31)
Sh1-FRBC-M80	175.86 (6.48)	185.08 (12.06)	1.05 (5.24)	0.9 (-17.49)	1.49 (12.77)	21.4 (-35.74)
Sh2-CC-M60	113.91	136.41	1.20	1.43	1.88	21.20
Sh2-BC-M60	160.16 (40.61)	196.70 (44.20)	1.23 (2.55)	1.53 (6.45)	2.72 (44.68)	58.20 (174.53)
Sh2-FRC-M60	113.90 (-0.01)	146.99 (7.76)	1.29 (7.76)	1.43 (-0.19)	2.03 (7.71)	23.20 (9.43)
Sh2-FRBC-M60	139.53 (22.50)	178.57 (30.91)	1.28 (6.87)	1.51 (4.97)	2.46 (30.83)	34.70 (63.68)
Sh2-CC-M80	126.72	164.22	1.30	1.50	2.27	35.40
Sh2-BC-M80	131.72 (3.95)	166.72 (1.52)	1.27 (-2.33)	1.77 (18.00)	2.30 (1.52)	33.90 (-4.24)
Sh2-FRC-M80	118.9 (-6.17)	168.51 (2.61)	1.42 (9.36)	1.81 (20.65)	2.32 (2.56)	35.70 (0.85)
Sh2-FRBC-M80	130.43 (2.93)	181.54 (10.55)	1.39 (7.40)	1.83 (21.99)	2.50 (10.34)	34.4 (-2.82)

3.1 Cracking Patterns

Multi-cracks were observed in the presence of fibers and bacterial additions. The propagated flexure cracks at mid-span of the L1, L2, Sh1, and Sh2 beams are represented in Figure 6, Figure 7, Figure 8, and Figure 9, respectively. The crack propagation for both slender and short beams observed at mid-span where all beams tend to fail due to the flexural. The orientations of the cracks were vertical in the mid-span bottom region and lightly inclined outward, in which the steel reinforcements will distribute cracks along the damage zone. The FRC beams did exhibit distributed flexural cracking before the first diagonal shear crack propagation due to the increased confining of the fibers around the steel bars. These results are broadly consistent with the major trends of experimental observations in the literature (Furlan Jr and de Hanai, 1997).

Incorporating bacillus subtilis bacteria at optimum dosage into M60 and M80 concrete strengthened with macro synthetic fiber transforms the unstable crack propagation into a controlled crack growth with more warning signs than conventional concrete. Also, the sudden failure could be eliminated by combining the macro synthetic fiber and bacteria as an internal reinforcement self-repairing technique. Hence, the enhancement of structural behavior such as flexural strength, deformation capacity, and ductility could be achieved for concrete structures.

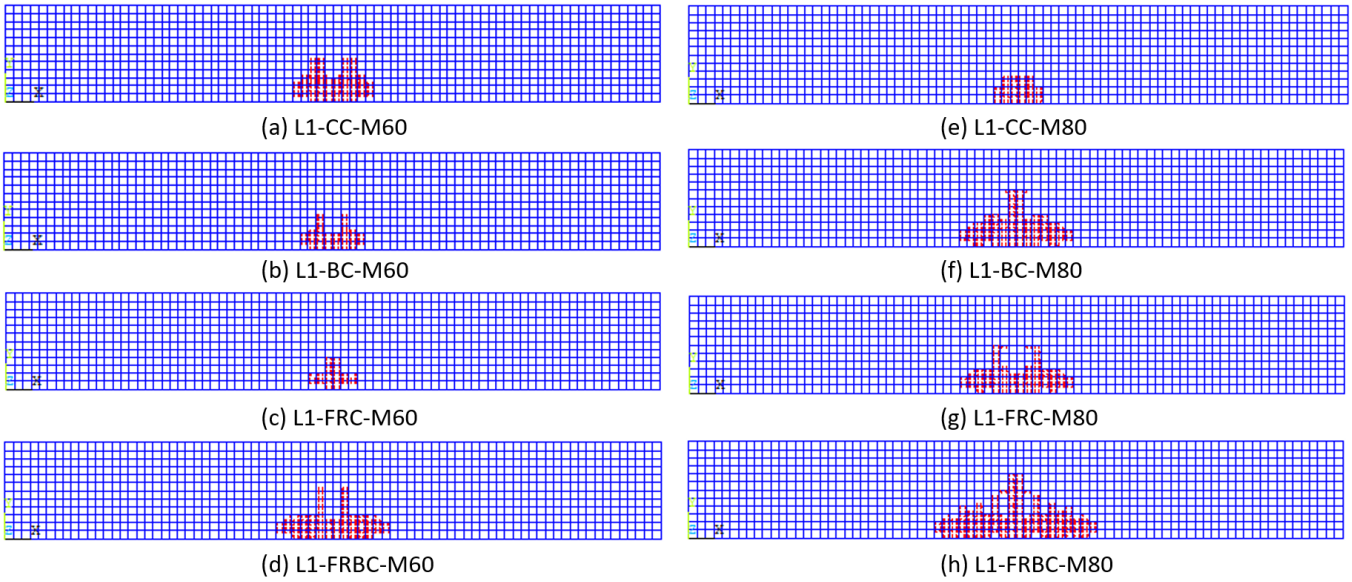

Figure 6: Failure Flexure Cracks Propagation Observed at Mid-Span of Beams: (a) L1-CC-M60, (b) L1-BC-M60, (c) L1-FRC-M60, (d) L1-FRBC-M60, (e) L1-CC-M80, (f) L1-BC-M80, (g) L1-FRC-M80 and (h) L1-FRBC-M80.

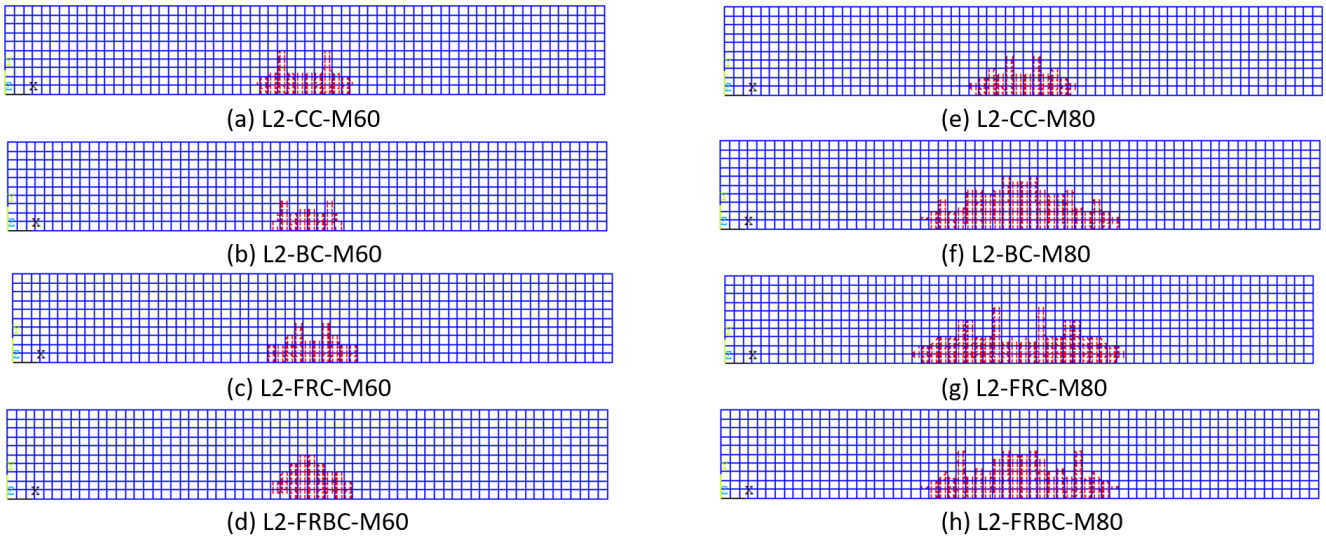

Figure 7: Failure Flexure Cracks Propagation Observed at Mid-Span of Beams: (a) L2-CC-M60, (b) L2-BC-M60, (c) L2-FRC-M60, (d) L2-FRBC-M60, (e) L2-CC-M80, (f) L2-BC-M80, (g) L2-FRC-M80 and (h) L2-FRBC-M80.

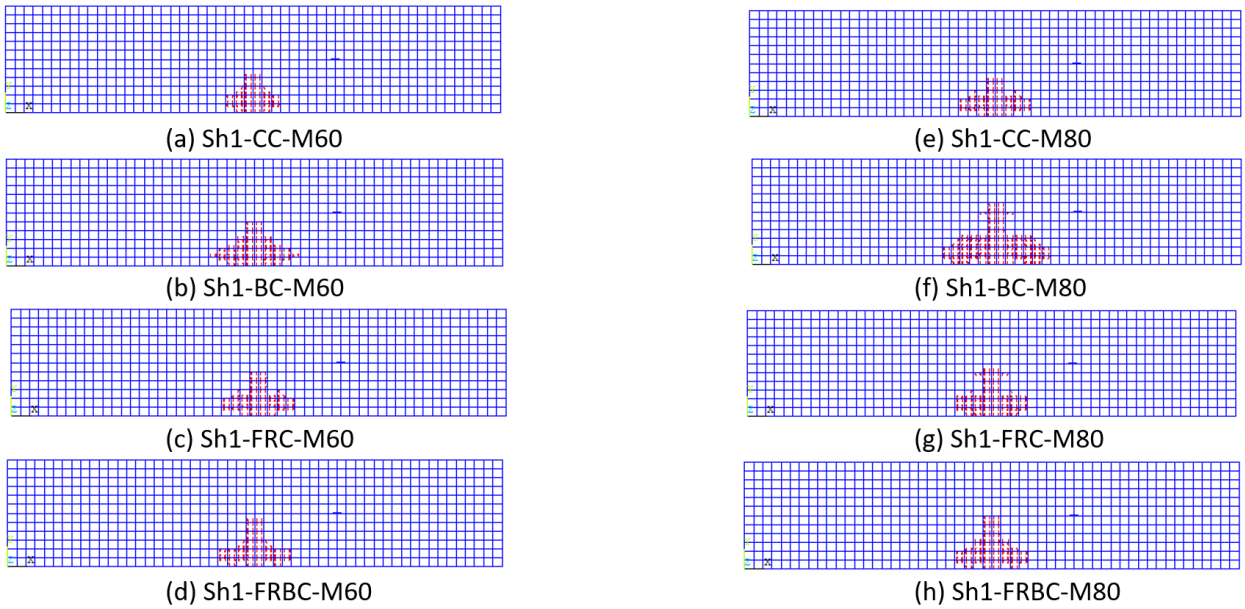

Figure 8: Failure Flexure Cracks Propagation Observed at Mid-Span of Beams: (a) Sh1-CC-M60, (b) Sh1-BC-M60, (c) Sh1-FRC-M60, (d) Sh1-FRBC-M60, (e) Sh1-CC-M80, (f) Sh1-BC-M80, (g) Sh1-FRC-M80 and (h) Sh1-FRBC-M80.

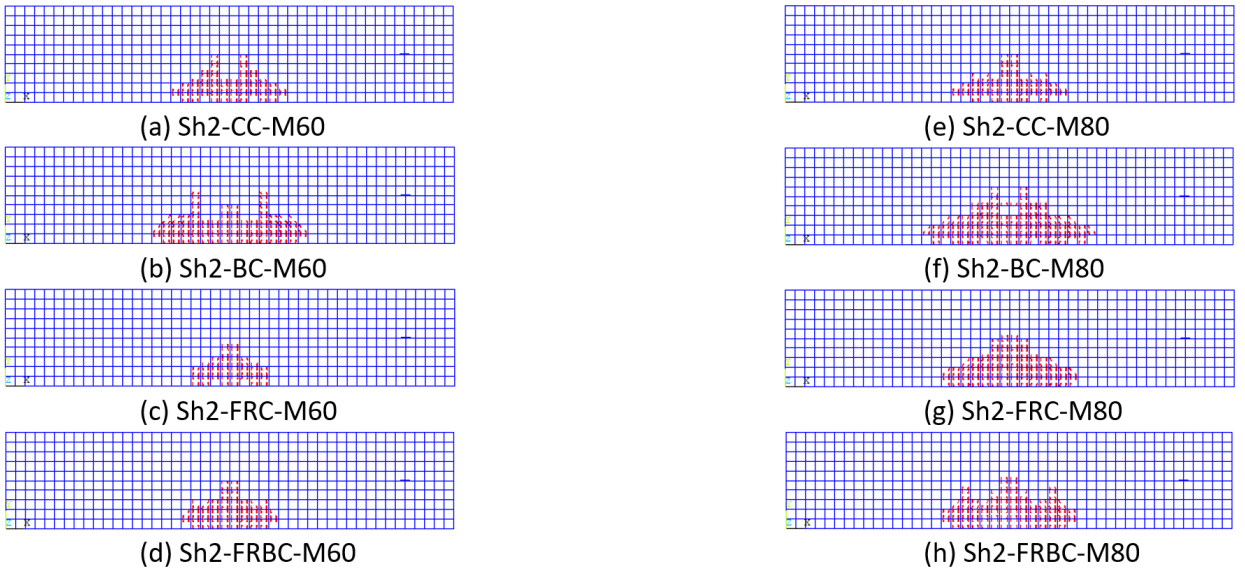

Figure 9: Failure Flexure Cracks Propagation Observed at Mid-Span of Beams: (a) Sh2-CC-M60, (b) Sh2-BC-M60, (c) Sh2-FRC-M60, (d) Sh2-FRBC-M60, (e) Sh2-CC-M80, (f) Sh2-BC-M80, (g) Sh2-FRC-M80 and (h) Sh2-FRBC-M80.

Figure 10 shows the value of mid-span vertical crack length at the ultimate load and the average crack length value for the different study specimens. For both fibrous M60 and M80 concrete, the FRBC average crack length at the ultimate load is more than that of FRC. This longer crack length with a bigger ultimate load means the more consumed amount of energy before failure. As a mutual benefit status, the reduced crack widths by fibers require fewer healing products to fill. Also, the healed crack by bacterial participation on the micro-scale increases the fiber embedment length. Consequently, the remarkable enhancement of the FRBC performance could be achieved among all fibers bridging cross cracks on the macro-scale of the composite. This observation is broadly consistent with the literature trend (Nili and Afroughsabet, 2010; Di Maida et al., 2018; Vijay and Murmu, 2019).

3.2 Bacterial Self-Repairing Influence

Moreover, the significance level was determined using the statistical analysis of variance (ANOVA) method to compare means and study parameters effect on the performance. The enhancement percentage related to associated CC in the target mechanical performance of different matrix types FRC, BC, and FRBC is illustrated in Figure 11. The relative change results showed that the influence of bacterial participation in fibrous concrete was more pronounced than the individual addition of bacteria or fibers in beams. The results of the test hypothesis, including a 95% confidence interval, showed that the FRBC had more mean significant enhancement in the initial cracking load P_{cr}, the ultimate load P_u, and the moment capacity ratio RM with a range of (6-21%), (20-42%), and (8-23%), respectively. Also, the relative enhancements in shear stress and toughness for FRC beams are more pronounced than BC beams. This confirms that fiber incorporation plays a bigger influence in improving concrete shear performance up to 80% as shown in Figure 11. These results are broadly consistent with the major trends of experimental observations in the literature. The macro fibers made remarkable improvements in beam shear strength by 30% (Altoubat et al., 2009; Li et al., 1992) and reach 65% using new generation macro synthetic fibers (Hasan et al., 2011; Kirsanov and Stolyarov, 2018).

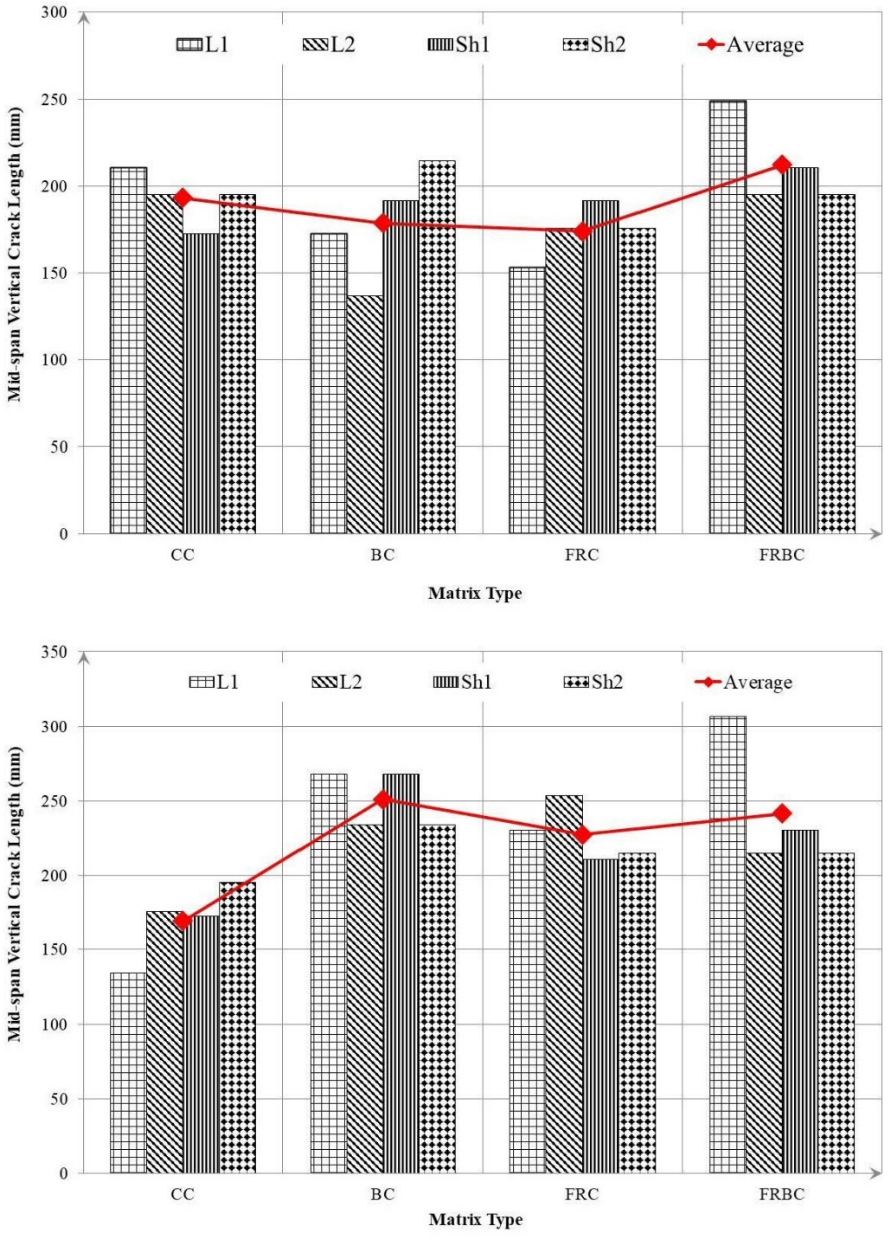

Figure 10: Value of Mid-Span Vertical Crack Length for different Matrix Types of Concrete Grades: (a) M60 and (b) M80.

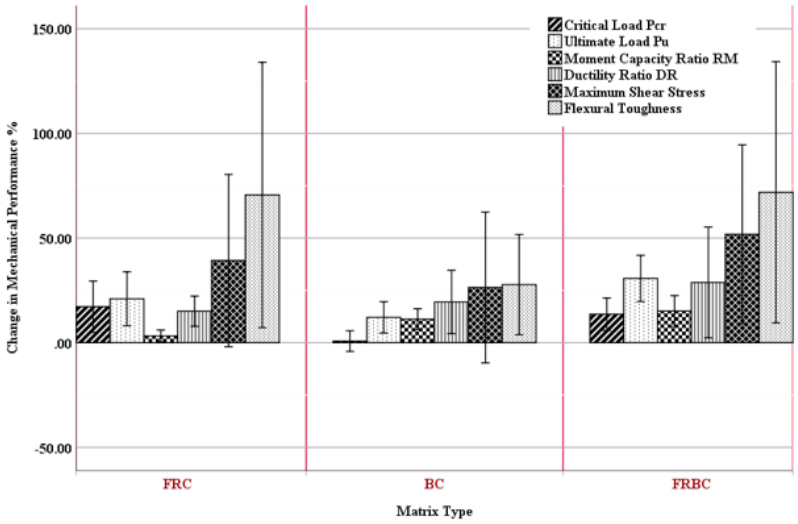

Figure 11: Analysis of the Enhancement Percentage in Target Mechanical Performance of Different Matrix Types.

3.3 Geometrical Parameters Influence

The enhancement percentage related to associated CC in the target mechanical performance of different model types L1, L2, Sh1, and Sh2 is as shown in Figure 12. The relative change results showed that the influence of fiber and bacteria addition in the slender beams was more pronounced than the short beams. The results of the test hypothesis including all matrix types showed that the L1 had more significant enhancement in the maximum shear strength v_{fc}.

3.4 Concrete Grade Influence

Figure 13 illustrates the enhancement percentage related to associated CC in the target mechanical performance of M60 and M80 concrete grade. The relative change results showed that the influence of fiber and bacteria addition in the M80 was more pronounced than in M60. The moment capacity ratio RM and the ductility ratio DR of M80 had more significant enhancement with a range of (5-18%) and (12-44%), respectively.

The addition of low modulus synthetic fiber and bacteria increased flexure strength, toughness, and residual load-carrying capacity due to high crack widths. However, the initial cracking load, ultimate load, and flexural toughness do not follow the trend of gradually increasing with the increased concrete grade. The results of the test hypothesis showed that the M60 had more mean significant enhancement in the initial cracking load, the ultimate load, and the flexural toughness with a range of (11-27%), (20-37%), and (47-130%), respectively. However, a dual-component improver has a higher synergistic effect, this improvement could not treat the high brittleness of the M80 concrete grade.

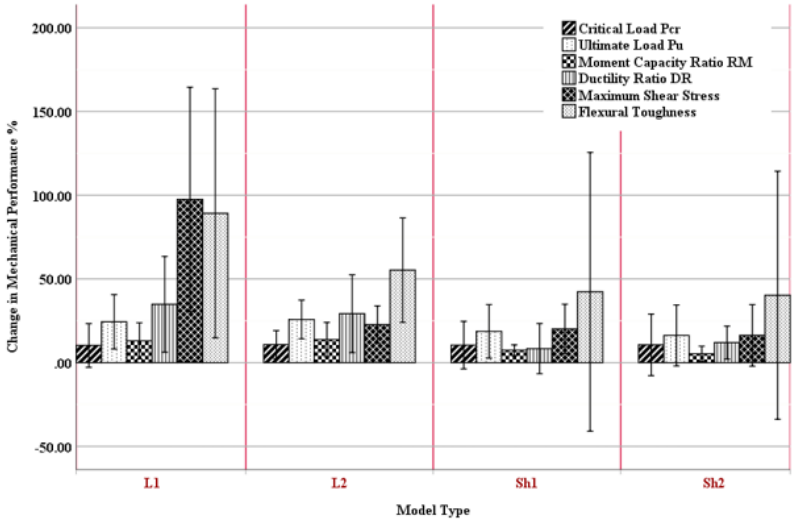

Figure 12: Analysis of the Enhancement Percentage in Target Mechanical Performance of Different Geometry Model Types.

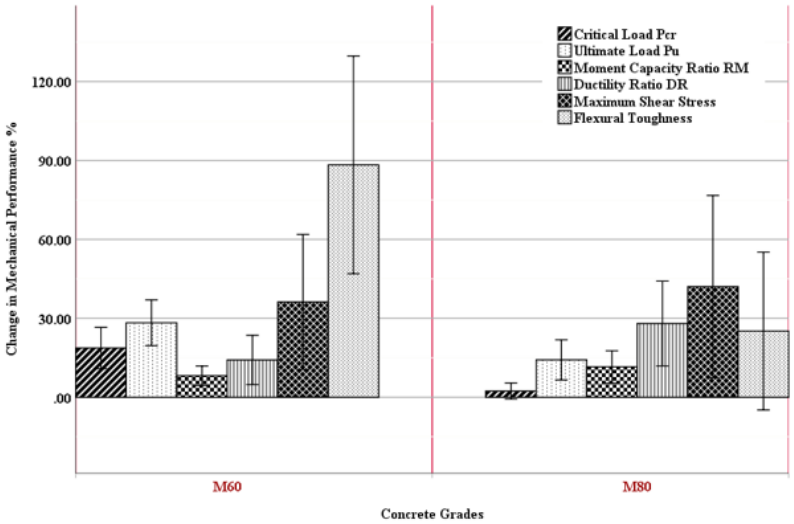

Figure 13: Analysis of the Enhancement Percentage in Target Mechanical Performance of Different Concrete Grade.

4 CONCLUSIONS

This paper presents a 3-point bending static loading numerical test. A database comprising 32 beams was assembled for evaluating the early-age enhancement in the predictive performance of Fiber-Reinforced Bacterial Concrete (FRBC) beams. The findings of the research are quite convincing, and thus the following conclusions can be drawn:

1. The bacterial participation and macro fiber addition, as a dual-component improver, presents a controlled crack growth with more warning signs than conventional concrete. For both fibrous M60 and M80 concrete, the FRBC average crack length at the ultimate load is more than that of FRC.
2. The results showed that the FRBC beams had more significant enhancement in the initial cracking load, the ultimate load, and the moment capacity ratio to associated conventional concrete. Also, the results provided that fiber incorporation plays a bigger influence than bacterial participation in improving concrete shear performance.
3. The study demonstrates that the incorporation of bacteria can increase the influence in the moment capacity ratio more than the single incorporation of macro fibers. Moreover, the inclusion of fibers plays the most dominant role in the enhancement of the initial cracking load, the ultimate load, and the flexural toughness.
4. Moreover, the enhancement influence of fiber and bacteria was more pronounced in the M80 beams moment capacity ratio and ductility ratio than that of M60 beams. However, the enhancement of initial cracking load, ultimate load, and flexural toughness was more pronounced in the M60 beams. Hence, the selection of the concrete grade should be suitable for the type of capacities enhancement required to the specific structural application.
5. For achieving sustainable development goals and greening the building industry, the internal reinforcement self-repairing technique is a promising novel technique. The structural design can take full advantage of the early-age high mechanical performance for preventing code driving deterioration factors.

Author's Contribuitions: Conceptualization, A Ghoniem and H Hassan; Methodology, A Ghoniem, H Hassan and L Aboul-Nour; Software and Formal anlysis, A Ghoniem; Investigation, A Ghoniem and L Aboul-Nour; Writing - original draft, A Ghoniem; Writing - review & editing, A Ghoniem; Visualization, A Ghoniem; Supervision, H Hassan and L Aboul-Nour.

Editor: Marcílio Alves

References

Alberti M., Enfedaque A., Gálvez J. and Picazo A. (2020). Recent advances in structural fibre-reinforced concrete focused on polyolefin-based macro-synthetic fibres. Materiales de Construcción 70 (337): 206, https://doi.org/10.3989/mc.2020.12418

Altoubat S., Yazdanbakhsh A. and Rieder K.-A. (2009). Shear behavior of macro-synthetic fiber-reinforced concrete beams without stirrups. ACI Materials Journal 106 (4): 381-389, https://doi.org/10.14359/56659

Athiyamaan V. and Ganesh G. M. (2017). Statistical and detailed analysis on fiber reinforced self-compacting concrete containing admixtures-A state of art of review. IOP Conf. Ser. Mater. Sci. Eng 263: 032037, https://doi.org/10.1088/1757-899X%2F263%2F3%2F032037

Ayub T., Khan S. U. and Shafiq N. (2018). Flexural modelling and finite element analysis of FRC beams reinforced with PVA and basalt fibres and their validation. Advances in Civil Engineering 2018: 1-18, https://doi.org/10.1155/2018/8060852

Ayub T., Shafiq N. and Nuruddin M. F. (2014). Stress-strain response of high strength concrete and application of the existing models. Research Journal of Applied Sciences, Engineering and Technology 8 (10): 1174-1190, https://doi.org/10.19026/rjaset.8.1083

Carnovale D. J. (2013). Behaviour and analysis of steel and macro-synthetic fibre reinforced concrete subjected to reversed cyclic loading: a pilot investigation. MSc Thesis, University of Toronto, pp. 138-167.

Carreira D. J. and Chu K.-H. (1985). Stress-strain relationship for plain concrete in compression. Journal Proceedings 82 (6): 797-804, https://doi.org/10.14359/10390

Di Maida P., Sciancalepore C., Radi E. and Bondioli F. (2018). Effects of nano-silica treatment on the flexural post cracking behaviour of polypropylene macro-synthetic fibre reinforced concrete. Mechanics Research Communications 88: 12-18, https://doi.org/10.1016/j.mechrescom.2018.01.004

Feng J., Su Y. and Qian C. (2019). Coupled effect of PP fiber, PVA fiber and bacteria on self-healing efficiency of early-age cracks in concrete. Construction and Building Materials 228: 116810, https://doi.org/10.1016/j.conbuildmat.2019.116810

Furlan Jr S. and de Hanai J. B. (1997). Shear behaviour of fiber reinforced concrete beams. Cement and concrete composites 19 (4): 359-366, https://doi.org/10.1016/S0958-9465%2897%2900031-0

Ganesh A. C., Muthukannan M., Malathy R. and Babu C. R. (2019). An Experimental Study on Effects of Bacterial Strain Combination in Fibre Concrete and Self-Healing Efficiency. Ksce Journal of Civil Engineering 23: 4368-4377, https://doi.org/10.1007/s12205-019-1661-2

Ghoneim A., Hassan H. and Aboul-Nour L. (2020). Self-repairing polyethylene fiber-reinforced-concrete with bacillus subtilis bacteria a review. International Journal of Engineering & Technology 9 (2): 437-447, http://dx.doi.org/10.14419/ijet.v9i2.30172

Griño A. A., Daly M., Klarissa M. and Ongpeng J. M. C. (2020). Bio-Influenced Self-Healing Mechanism in Concrete and Its Testing: A Review. Applied Sciences 10 (15): 5161, https://doi.org/10.3390/app10155161

Guerini V., Conforti A., Plizzari G. and Kawashima S. (2018). Influence of steel and macro-synthetic fibers on concrete properties. Fibers 6 (3): 1-14, https://doi.org/10.3390/fib6030047

Hasan A., Maroof N. and Ibrahim Y. (2019). Effects of polypropylene fiber content on strength and workability properties of concrete. Polytechnic Journal 9 (1): 7-12, https://doi.org/10.25156/ptj.v9n1y2019.pp7-12

Hasan M., Afroz M. and Mahmud H. (2011). An experimental investigation on mechanical behavior of macro synthetic fiber reinforced concrete. International Journal of Civil and Environmental Engineering 11 (3): 18-23

Hizami Abdullah M. A., Harmiza Abdullah N. A. and Tompang M. F. (2018). Development and Performance of Bacterial Self-healing Concrete - A Review. IOP Conference Series: Materials Science and Engineering 431: 062003, https://doi.org/10.1088/1757-899X%2F431%2F6%2F062003

Júnior L. Á. O., Borges V. E. S., Danin A. R., Machado D. V. R., Araújo D., Debs M. and Rodrigues P. F. (2010). Stress-strain curves for steel fiber-reinforced concrete in compression. Matéria (Rio de Janeiro) 15 (2): 260-266, https://doi.org/10.1590/S1517-70762010000200025

Karimi N. and Mostofinejad D. (2020). Bacillus subtilis bacteria used in fiber reinforced concrete and their effects on concrete penetrability. Construction and Building Materials 230: 117051, https://doi.org/10.1016/j.conbuildmat.2019.117051

Kirsanov A. and Stolyarov O. (2018). Mechanical properties of synthetic fibers applied to concrete reinforcement. Magazine of Civil Engineering 82 (6): 15-23, https://doi.org/10.18720/mce.80.2

Li L., Zheng Q., Li Z., Ashour A. and Han B. (2019). Bacterial technology-enabled cementitious composites: A review. Composite structures 225: 111170, https://doi.org/10.1016/J.COMPSTRUCT.2019.111170

Li V. C., Ward R. and Hamza A. M. (1992). Steel and synthetic fibers as shear reinforcement. ACI Materials Journal 89 (5): 499-508, https://doi.org/10.14359/1822

Liao W.-C., Perceka W. and Liu E.-J. (2015). Compressive stress-strain relationship of high strength steel fiber reinforced concrete. Journal of Advanced Concrete Technology 13 (8): 379-392, https://doi.org/10.3151/jact.13.379

Lu Z.-H. and Zhao Y.-G. (2010). Empirical stress-strain model for unconfined high-strength concrete under uniaxial compression. Journal of Materials in Civil Engineering 22 (11): 1181-1186, https://doi.org/10.1061/%28ASCE%29MT.1943-5533.0000095

MacGregor J. G. and Wight J. K. (2012). Reinforced Concrete: Mechanics and Design, Section 6–3, 6th ed., New Jersey, Pearson.

Micelli F., Candido L., Vasanelli E., Aiello M. A. and Plizzari G. (2019). Effects of short fibers on the long-term behavior of RC/FRC beams aged under service loading. Applied Sciences 9 (12): 1-13, https://doi.org/10.3390/app9122540

Nili M. and Afroughsabet V. (2010). Combined effect of silica fume and steel fibers on the impact resistance and mechanical properties of concrete. International Journal of Impact Engineering 37 (8): 879-886, https://doi.org/10.1016/j.ijimpeng.2010.03.004

Oh J. H. (2011). Uniaxial behaviour of steel fiber reinforced concrete. South Korea, MSc thesis, Seoul National University.

Rao M. V. S., Reddy V. S. and Sasikala C. (2017). Performance of microbial concrete developed using bacillus subtilus JC3. Journal of The Institution of Engineers (India): Series A 98 (4): 501-510, https://doi.org/10.1007/s40030-017-0227-x

Termkhajornkit P., Nawa T., Yamashiro Y. and Saito T. (2009). Self-healing ability of fly ash–cement systems. Cement and concrete composites 31 (3): 195-203, https://doi.org/10.1016/j.cemconcomp.2008.12.009

Thomas J. and Ramaswamy A. (2006). Finite element analysis of shear critical prestressed SFRC beam. Computer and Concrete 3 (1): 65-77, https://doi.org/10.12989/cac.2006.3.1.065

Thomas J. and Ramaswamy A. (2007). Mechanical properties of steel fiber-reinforced concrete. Journal of Materials in Civil Engineering 19 (5): 385-392, https://doi.org/10.1061/%28ASCE%290899-1561%282007%2919%3A5%28385%29

Vijay K. and Murmu M. (2019). Self-repairing of concrete cracks by using bacteria and basalt fiber. SN Applied Sciences 1 (11): 1344, https://doi.org/10.1007/s42452-019-1404-5

Wiktor V. and Jonkers H. M. (2011). Quantification of crack-healing in novel bacteria-based self-healing concrete. Cement and concrete composites 33 (7): 763-770, https://doi.org/10.1016/j.cemconcomp.2011.03.012

Won J.-P., Lim D.-H. and Park C.-G. (2006). Bond behaviour and flexural performance of structural synthetic fibre-reinforced concrete. Magazine of Concrete Research 58 (6): 401-410, https://doi.org/10.1680/macr.2006.58.6.401

Zhang W., Zheng Q., Ashour A. and Han B. (2020). Self-healing cement concrete composites for resilient infrastructures: A review. Composites Part B-engineering 189: 107892, https://doi.org/10.1016/j.compositesb.2020.107892